Development 136, 2893-2902 (2009) doi:10.1242/dev.036103

Graded Egfr activity patterns the *Drosophila* eggshell independently of autocrine feedback

Jean-François Boisclair Lachance, Mariana Fregoso Lomas, Aliaa Eleiche, Phoenix Bouchard Kerr and Laura A. Nilson*

The pattern of the *Drosophila* eggshell is determined by the establishment of a complex and stereotyped pattern of cell fates in the follicular epithelium of the ovary. Localized activation of the Epidermal growth factor receptor (Egfr) is essential for this patterning. Modulation of Egfr pathway activity in time and space determines distinct fates at their appropriate locations, but the details of how Egfr signaling is regulated and how the profile of Egfr activity corresponds to cell fate remain unclear. Here we analyze the effect of loss of various Egfr regulators and targets on follicle cell patterning, using a marker for follicle cell fate, and on the mature eggshell phenotype, using a novel eggshell marker. We show, contrary to current patterning models, that feedback regulation of Egfr activity by the autocrine ligand Spitz and the inhibitor Argos is not necessary for patterning. Given the cell-autonomous nature of the mutant phenotypes we observed, we propose instead that the pattern of cell fates is generated by spatial information derived directly from the germline ligand Gurken, without a requirement for subsequent patterning by diffusible Egfr regulators in the follicular epithelium.

KEY WORDS: *Drosophila*, Epidermal growth factor receptor, Oogenesis, Epithelial patterning

INTRODUCTION

The follicular epithelium of the *Drosophila* ovary provides a well-characterized genetic system that allows a detailed analysis of how spatial and temporal regulation of conserved signaling pathways can generate a complex pattern of cell fate (Berg, 2005; Horne-Badovinac and Bilder, 2005; Nilson and Schupbach, 1999). The follicular epithelium surrounds the germline of each developing egg chamber and ultimately produces the eggshell (Spradling, 1993). The patterning of the follicular epithelium is thus reflected in the eggshell it produces, which exhibits pronounced axial asymmetries in its shape and in the presence of specialized structures, such as two dorsal respiratory appendages.

Central to the patterning of this tissue are two inductive signals: an Epidermal growth factor receptor (Egfr) ligand encoded by the *gurken* (*grk*) gene, and Decapentaplegic (Dpp), a member of the bone morphogenetic protein group of transforming growth factor β signaling molecules (Berg, 2005; Horne-Badovinac and Bilder, 2005; Nilson and Schupbach, 1999). In mid-oogenesis, Grk is localized to the dorsal side of the oocyte, where it induces spatially restricted activation of Egfr in the overlying follicle cells. This localized Egfr activation is essential for determination of the two distinct primordia that produce the two eggshell appendages and for their proper positioning along the dorsal-ventral (DV) axis (Neuman-Silberberg and Schupbach, 1993; Neuman-Silberberg and Schupbach, 1996; Schupbach, 1987). Dpp is produced by the anterior-most follicle cells, which overlie the nurse cells, and regulates patterning along the anterior-posterior (AP) axis (Dequier et al., 2001; Twombly et al., 1996). The combined action of these two ligands during these stages establishes and positions the appendage primordia (Chen and Schupbach, 2006; Deng and Bownes, 1997; Peri and Roth, 2000; Shravage et al., 2007).

Department of Biology, McGill University, 1205 Doctor Penfield Avenue, Montréal, Quebec H3A 1B1, Canada.

*Author for correspondence (laura.nilson@mcgill.ca)

Accepted 19 June 2009

An interesting aspect of this patterning process is that the single Grk/Egfr signal initially reaches a broad field of dorsal anterior follicle cells, yet ultimately leads to the establishment within this field of two dorsolateral appendage primordia separated by a distinct dorsal midline region. This pattern has been proposed to arise through a feedback loop in which the initial Grk/Egfr signal induces the expression of the Rhomboid (Rho) intracellular protease, leading to the production of a second Egfr ligand, Spitz (Spi), which amplifies the initial Egfr activation. According to this model, high levels of Egfr activity at the dorsal midline in turn induce the expression of Argos (Aos), a secreted inhibitor of Spi, leading to decreased Egfr activity in this region and accounting for the observed decrease in activated MAPK (Rolled – FlyBase) at the dorsal midline (Klein et al., 2004; Wasserman and Freeman, 1998). Negative-feedback regulation is thus proposed to split the initial field of Grk/Egfr signaling, creating a low-signaling region that generates the appendage-free dorsal midline domain that separates the two appendage primordia (Wasserman and Freeman, 1998).

Much of our understanding of follicle cell patterning has been derived from analyzing eggshell patterning defects. Looking directly at the follicular epithelium during oogenesis, however, reveals that some aspects of this process remain unclear. For example, although downregulation of Egfr activity by Aos at the dorsal midline has been proposed to split the initial dorsal field of Egfr activity into two dorsolateral peaks, comparing the spatial and temporal profile of MAPK activation with that of an appendage fate marker shows, instead, that high (not low) Egfr activity is associated with the appearance of dorsal midline fate; decreased Egfr activity in these cells is detected only later, after the midline fate is established (Kagesawa et al., 2008; Peri et al., 1999). Also inconsistent with an Aos-mediated negative-feedback model is the observation that midline *aos* expression is observed after, not before, the establishment of the dorsal midline region (Wasserman and Freeman, 1998; Yakoby et al., 2008a). Such apparent discrepancies suggest that current models of Egfr signaling and eggshell patterning are incomplete.

Here we investigate the contribution of several regulators and effectors of Egfr signaling to the patterning of the follicular epithelium. We directly analyze follicle cell fate by examining the effect of mutant follicle cell clones on the establishment and positioning of the appendage primordia, enabling characterization of patterning defects with a resolution not possible from analysis of the mature eggshell. Since defects could potentially arise downstream of patterning, for example during appendage morphogenesis, we also look at the eggshells produced by females with follicle cell clones. Analyzing such eggshells has been inherently problematic because mosaics produce mixed populations of eggs, and there has been no easily detectable marker to indicate which eggs are derived from egg chambers with completely mutant follicular epithelia. We therefore developed a novel eggshell marker system that utilizes a follicle cell-dependent dominant female-sterile mutation to allow eggshells produced by mutant epithelia to be reliably identified, analogous to the *P[ovoD1]* system for marking germline clones (Chou and Perrimon, 1996). This tool has enabled us to correlate definitively the effect of mutations on cell fate patterning with their effect on the resulting eggshell.

Unexpectedly, our data show that the Spi/Aos feedback loop is not required to establish the normal pattern of follicle cell fates or for production of normally patterned eggshells. By contrast, we show that Mirror (Mirr) and Pointed (Pnt), transcription factors that function downstream of Egfr signaling, and Sprouty (Sty), an inhibitor of receptor tyrosine kinase (RTK) signaling, play distinct roles in follicle cell patterning. Mirr is required for the establishment of all dorsal anterior fates, whereas Pnt is required to generate the dorsal midline region. Sty restricts the width of the midline region, consistent with a role in negative regulation of Egfr signaling. Importantly, each transcription factor is required cell-autonomously. Together, these data suggest that the DV pattern of follicle cell fates is determined directly by the Grk gradient, without a requirement for intervening autocrine feedback.

MATERIALS AND METHODS

Generation of mosaics

Mosaic females were generated as described (Laplante and Nilson, 2006), using standard FRT sites and genotypic markers obtained from the Bloomington Stock Center. The mutant strains used were: *rho*^{6} *P{neoFRT}80B*, *rho*^{7M43} *P{neoFRT}80B* (gift from S. Roth) (Wasserman and Freeman, 1998), *aos*$^{\Delta 7}$ *P{neoFRT}80B* (gift from N. S. Moon) (Voas and Rebay, 2003), *spi*^{1} *P{neoFRT}40A*, *spi*^{3} *P{neoFRT}40A* (gift from T. Schüpbach, Princeton University), *P{neoFRT}82B cic*^{U6} (Goff et al., 2001), *P{neoFRT}82B pnt*$^{\Delta 78}$ (O'Neill et al., 1994), *P{neoFRT}82B pnt*$^{\Delta 88}$ (gift from H. Ruohola-Baker) (Scholz et al., 1993), *mirr*^{e48} *P{neoFRT}80B* (gift from S. Roth), *mirr*$^{l(3)6D1}$ (Jordan et al., 2000), *sty*$^{\Delta 5}$ *P{neoFRT}80B*, *sty*^{226} *P{neoFRT}80B*, *P{neoFRT}42D wind*^{RP54} (Nilson and Schupbach, 1998) and *pip*^{664} *P{neoFRT}80B* (L.A.N., unpublished). The presence of *rho*, *spi* and *aos* mutations on these chromosomes was confirmed by complementation test. Additionally, *rho* mutations were confirmed by the generation of wing clones with loss of wing veins, which is characteristic of loss of *rho* (Sturtevant et al., 1993). *spi*^{1} is also known as *spi*^{A14} and *spi*^{3} as *spi*^{OE72}.

Generation of FRT-*P[decDN]* chromosomes

The *P[decDN]* transgene consists of a *pCaSpeR4* P-element vector containing a cDNA encoding a version of the Dec-1 fc106 pro-protein with an engineered deletion of the s20 region (fc106ΔV288-E473) (Spangenberg and Waring, 2007). Chromosomes bearing an FRT site and a *P[decDN]* insertion were generated by standard injection of the *pCaSpeR4-decDN* plasmid into strains containing existing FRT transgenes (Xu and Rubin, 1993) or by P-element-mediated male recombination (*P{neoFRT}42D P[decDN]77.1*) (Preston and Engels, 1996). Strains that contained *P[decDN]* insertions, maintained FRT function, and exhibited complete penetrance of the *P[decDN]* collapsed egg phenotype were retained for use in mosaic studies.

Egg collection and phenotypic analysis using the *P[decDN]* marker

Mitotic recombination was induced as described (Laplante and Nilson, 2006) in females containing an FRT-*P[decDN]* chromosome in trans to a chromosome containing the same FRT and a mutation of interest. Eggs were collected on apple juice agar plates supplemented with dry yeast. The collapsed phenotype ranged in severity from completely collapsed eggshells to eggshells that retained a relatively normal three-dimensional shape but were translucent, often deformed, and tended to collapse upon storage at 4°C. For all genotypes, the data in Tables 1 and 2 were compiled from multiple independent trials.

Immunohistochemistry

Ovaries were fixed and stained as described previously (Laplante and Nilson, 2006). Primary antibodies used were mouse anti-BR-C core hybridoma supernatant 25E9.D7 (1:200, Developmental Studies Hybridoma Bank), rat anti-Ed (1:1000) (Laplante and Nilson, 2006) and rabbit anti-c-Myc supernatant sc-789 (1:200, Santa Cruz Biotechnology). Secondary antibodies (Molecular Probes) used were goat anti-mouse Alexa Fluor 555 (1:2000), goat anti-mouse Alexa Fluor 594 (1:1000), goat anti-rabbit Alexa Fluor 488 (1:2000) and goat anti-rat Alexa Fluor 647 (1:2000).

Microscopy and image analysis

Images were acquired using a Zeiss Axioplan 2 wide-field fluorescence microscope or a Zeiss LSM 510 confocal microscope (McGill Cell Imaging and Analysis Network Facility). Apart from minor adjustments to brightness and contrast in Figs 2 and 4, no image manipulations were performed. Measurements of inter-appendage distance represent the distance between the dorsal-most edges of the appendages. All measurements and cell counts are reported as mean ± s.e.

RESULTS

Loss of *rho*, *aos* or *spi* does not cause follicle cell patterning defects

The proposed role of Spi and Aos in eggshell patterning (Wasserman and Freeman, 1998) predicts that loss of *spi* or *rho* function will block amplification of the initial Grk/Egfr signal, resulting in a reduced domain of dorsal follicle cell fates, with reduced or absent dorsal midline fates and a single dorsally localized appendage primordium. Loss of *aos* function is predicted to eliminate the inhibition of Egfr signaling in the dorsal-most follicle cells, blocking the establishment of the dorsal midline region and yielding a single broad primordium.

To test these predictions, we generated follicle cell clones homozygous for mutant alleles of *spi*, *aos* or *rho*, and looked directly at follicle cell patterning using Broad Complex [BR-C; Broad (Br) – FlyBase] expression as a cell fate marker (Deng and Bownes, 1997; DiBello et al., 1991). In wild-type ovaries, BR-C protein expression is uniform in all follicle cells at early stages of oogenesis, but at early stage 10, BR-C becomes strongly reduced in a dorsal anterior T-shaped group of cells that will contribute to the eggshell operculum (Fig. 1A,A′, bars). Although indistinguishable in terms of BR-C expression, we will refer to the anterior portion of this 'T' as the operculum region and the dorsal portion as the dorsal midline region to reflect our observation (see below) that they are differentially sensitive to genetic manipulations. Slightly later, BR-C levels are elevated in the presumptive roof cells of the two appendage primordia (Fig. 1B,B′) (Deng and Bownes, 1997; Dorman et al., 2004; Tzolovsky et al., 1999). The remaining posterior and ventral cells exhibit lower, 'basal' BR-C levels.

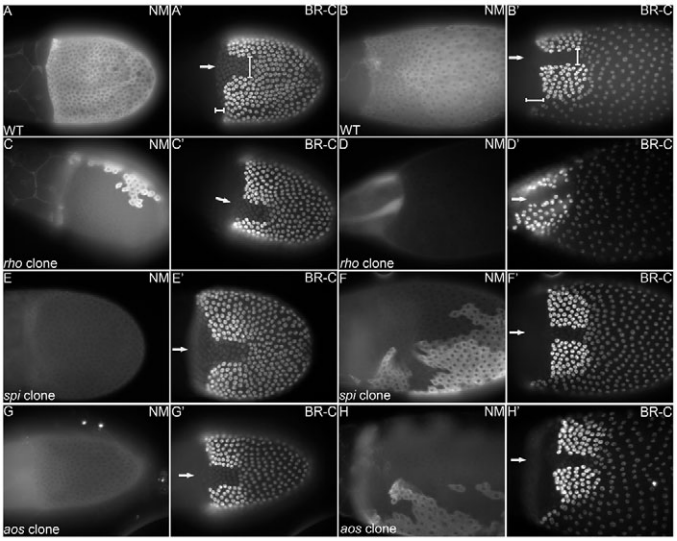

Fig. 1. *rho*, *spi* or *aos* mutant clones do not affect dorsal anterior follicle cell fates. *Drosophila* ovaries were stained for the N-Myc (NM) clone marker (Xu and Rubin, 1993) (A-H) and for BR-C expression (A′-H′). Anterior is to the left in all panels. Arrows indicate the dorsal midline position. WT refers to control egg chambers produced by mosaic females but lacking homozygous mutant clones. Bars in A′,B′ indicate the length of the operculum domain along the AP axis and the width of the midline domain along the DV axis. (**A**,**A′**) Stage 10B control egg chamber. (**B**,**B′**) Stage 12 control egg chamber. (**C**,**C′**) Stage 10B egg chamber with a nearly complete dorsal *rho* mutant clone. (**D**,**D′**) Stage 13 egg chamber with a complete *rho* mutant clone. (**E**,**E′**) Stage 10B egg chamber with all follicle cells mutant for *spi*. (**F**,**F′**) Stage 11 egg chamber with a *spi* clone nearly covering the entire dorsal anterior region. (**G**,**G′**) Stage 10B egg chamber with a complete *aos* mutant clone. (**H**,**H′**) Stage 12 egg chamber with a mutant clone of *aos* involving most of the dorsal anterior region.

Contrary to the above prediction, egg chambers with follicle cell clones homozygous for the amorphic rho^{7M43} allele exhibited a wild-type BR-C pattern, with a dorsal midline region of normal width (Fig. 1C-D′). This normal phenotype was observed even in egg chambers in which the follicular epithelium was composed entirely of *rho* mutant cells (23/23) (Fig. 1D′), and was completely penetrant (55/55). Normal BR-C expression was also evident at later stages of oogenesis when dorsal appendages were being formed (Fig. 1D,D′). Midline width was normal at these late stages, even though the epithelial morphogenesis associated with appendage formation can give the appearance of a reduced distance between the appendage primordia. We found the same lack of effect on BR-C expression for the rho^{6} allele (10/10). Consistent with our observations for *rho*, large *spi*-null mutant follicle cell clones had no effect on the pattern of BR-C expression (Fig. 1E-F′) (12/12 for spi^{1} and 12/12 for spi^{3}). Similarly, although loss of *aos* is predicted to abolish the appendage-free dorsal midline region, egg chambers with complete (Fig. 1G,G′) (11/11) or very large (Fig. 1H,H′) (16/16) clones homozygous for the amorphic $aos^{\Delta 7}$ allele displayed two normal domains of high BR-C expression separated by a clear midline region of normal width (3.8±0.2 cells versus 4.0±0.2 cells for non-mosaic egg chambers from the same females). Together, these data indicate that feedback modulation of Egfr signaling by Rho, Spi and Aos is not required for normal patterning of the follicular epithelium.

Establishing a novel dominant follicle cell-dependent female-sterile mutation as an eggshell marker

Although the above analysis showed no effect on BR-C expression, we asked whether *rho*, *spi* or *aos* mutant follicular epithelia exhibiting a normal BR-C expression pattern could nevertheless produce the previously reported eggshell appendage defects (Wasserman and Freeman, 1998). To identify which of the eggs produced by mosaic females were derived from egg chambers with homozygous mutant follicle cell clones, we developed a marker that incorporates information about the follicle cell genotype into the phenotype of the eggshell. This marker is a transgene bearing a dominant-negative form of the *defective chorion 1* (*dec-1*) gene, which is required in the follicle cells for eggshell integrity (Bauer and Waring, 1987; Hawley and Waring, 1988). The dominant-negative version, *P[decDN]*, bears an engineered deletion within the *dec-1* coding region that causes dominant female sterility and the production of dec-like collapsed eggs (Spangenberg and Waring, 2007). We reasoned that the *P[decDN]* transgene could function as a dominant genotypic marker for eggs derived from egg chambers with mutant follicle cell clones, analogous to the *ovoD* system for identification of eggs derived from mutant germline clones (Chou and Perrimon, 1992; Chou and Perrimon, 1996). Induction of FRT-mediated mitotic recombination in females transheterozygous for a mutation of interest and *P[decDN]* would generate egg chambers containing homozygous mutant follicle cells that lack *P[decDN]*. Eggs derived from egg chambers with large or complete mutant follicle cell clones, which lack *P[decDN]*, should therefore be readily identifiable because they would remain intact, whereas those produced by non-mutant follicular epithelia retaining *P[decDN]* would collapse.

Initial tests of this system showed that a fraction of the eggs produced by mosaic females bearing an FRT-*P[decDN]* chromosome in trans to a wild-type FRT chromosome remained intact, whereas non-mosaic females bearing the same FRT-*P[decDN]* chromosome produced only collapsed eggs, suggesting that the intact eggs were the product of egg chambers with homozygous follicle cell clones (Table 1). Moreover, all intact eggs produced by females mosaic for *P[decDN]* and a mutant allele of *capicua* (*cic*), which is required in the follicle cells for normal eggshell patterning (Atkey et al., 2006; Goff et al., 2001), exhibited the characteristic cic dorsalized eggshell phenotype (Table 1), confirming that this marker allows the selection of eggs derived from egg chambers with homozygous mutant follicle cell clones.

To determine whether intact eggs are derived exclusively from complete follicle cell clones, in which all follicle cells are homozygous mutant, or whether epithelia with partial clones can also produce intact eggs, we looked for localized defects in eggs produced by mosaic females. Intact eggshells produced by *cic* mosaic females exhibited no evidence of partial dorsalization (Table 1), demonstrating that they were produced by follicular epithelia with mutant clones involving at least the entire anterior region. We also generated females mosaic for *windbeutel* (*wind*; *wbl*) and *pipe* (*pip*) (Stein et al., 1991; Schupbach et al., 1991), as partial *wind* or *pip* clones cause localized dorsalization of the embryo (Nilson and Schupbach, 1998). However, all intact eggs produced by *wind* or *pip* mosaic females bearing the *P[decDN]* marker gave rise to embryos that were completely dorsalized (Table 1); no cases of localized dorsalization were observed. Although we cannot rule out the possibility that epithelia with small groups of *P[decDN]*-bearing follicle cells can produce non-collapsed eggshells, these data strongly suggest that only egg chambers with completely

Table 1. Validation of *P[decDN]* as an eggshell marker for follicle cell clones: frequency and expected phenotype of intact eggs recovered from control and mosaic females

Category	Genotype*	Total eggs	Intact % (*n*)	Expected phenotype % (*n*)
Non-mosaic†	*TM6B/FRT^{82B} P[decDN]140.1*	1751	0 (0)	n.a.
	TM3/FRT^{82B} P[decDN]140.1	1454	0 (0)	
	TM3/FRT^{82B} P[decDN]140.1	1383	0 (0)	
	TM6B/FRT^{82B} P[decDN]140.4	1105	0 (0)	
	TM3/FRT^{82B} P[decDN]140.4	685	0 (0)	
	TM3/FRT^{82B} P[decDN]140.6	1915	0 (0)	
	TM3/FRT^{82B} P[decDN]140.7	1328	0 (0)	
	CyO/FRT^{42D} P[decDN]77.1	3414	0 (0)	
	CyO/FRT^{42D} P[decDN]77.1	4980	0 (0)	
	CyO/FRT^{42D} P[decDN]]217.1	2170	0.046 (1)	
	TM3/P[decDN]118.3 FRT^{80B}	3215	0 (0)	
	TM3/P[decDN]118.3 FRT^{80B}	2144	0 (0)	
Wild-type mosaic	*FRT^{82B}/FRT^{82B} P[decDN]140.1*	1447	5.4 (78)	100 (207)‡
	FRT^{82B}/FRT^{82B} P[decDN]140.1	919	3.6 (33)	
	FRT^{82B}/FRT^{82B} P[decDN]140.4	920	7.9 (73)	
	FRT^{82B}/FRT^{82B} P[decDN]140.7	817	2.8 (23)	
cic mosaic	*FRT^{82B} cic^{U6}/FRT^{82B} P[decDN]140.1*	745	0.67 (5)§	100 (63)¶
	FRT^{82B} cic^{U6}/FRT^{82B} P[decDN]140.4	1400	1.1 (15)§	
	FRT^{82B} cic^{U6}/FRT^{82B} P[decDN]140.4	2106	0.24 (5)§	
	FRT^{82B} cic^{U6}/FRT^{82B} P[decDN]140.6	1630	0.18 (3)§	
	FRT^{82B} cic^{U6}/FRT^{82B} P[decDN]140.6	2112	0.62 (13)§	
	FRT^{82B} cic^{U6}/FRT^{82B} P[decDN]140.6	1230	0.24 (3)§	
	FRT^{82B} cic^{U6}/FRT^{82B} P[decDN]140.7	1755	0.57 (10)§	
	FRT^{82B} cic^{U6}/FRT^{82B} P[decDN]140.7	2574	0.35 (9)§	
Wild-type mosaic	*FRT^{42D}/FRT^{42D} P[decDN]77.1*	1617	3.7 (60)	100 (126)**
	FRT^{80B}/P[decDN]118.3 FRT^{80B}	n.d.	n.d. (113)	
wind mosaic	*FRT^{42D} wind^{RP54}/FRT^{42D} P[decDN] 77.1*	3177	3.4 (107)	100 (641)††
	FRT^{42D} wind^{RP54}/FRT^{42D} P[decDN] 77.1	3480	19.0 (662)	
	FRT^{42D} wind^{RP54}/FRT^{42D} P[decDN] 217.1	1608	6.7 (108)	
pipe mosaic	*pip^{664} FRT^{80B}/P[decDN] 118.3 FRT^{80B}*	4644	10.7 (496)	100 (562)‡‡
	pip^{664} FRT^{80B}/P[decDN] 118.3 FRT^{80B}	3855	5.2 (202)	

*Some genotypes are repeated to indicate that the data were obtained in multiple independent trials.
†As non-mosaic controls for *P[decDN]* penetrance, we used female siblings of the mutant mosaic females.
‡Wild-type eggshell.
§Clone frequency is likely to be underestimated because eggs with cic phenotype often appear collapsed even when produced by homozygous (non-mosaic) females.
¶Dorsalized eggshell.
**Of 173 intact eggs, 126 were fertilized and 100% of the embryos were wild type.
††Of 877 intact eggs, 641 were fertilized and 100% of the embryos exhibited a D0 completely dorsalized phenotype.
‡‡Of 698 intact eggs, 562 were fertilized and 100% of the embryos exhibited a D0 completely dorsalized phenotype.
n.a., not applicable. Eggshell phenotype is only scored for intact eggs.
n.d., not determined.

homozygous mutant follicular epithelia can give rise to intact eggs. These data validate *P[decDN]* as an eggshell marker for complete follicle cell clones.

Loss of *rho*, *aos* or *spi* does not result in dorsal appendage defects

To ask whether *rho*, *spi* or *aos* play a role in eggshell patterning that is not reflected in the normal pattern of BR-C expression, we assessed the phenotype of eggshells produced by mosaic females bearing the *P[decDN]* marker. Consistent with their normal BR-C pattern (Fig. 1C-D′), virtually all intact eggs recovered from *rho^{7M43}*, *rho^{6}*, *spi^{1}*, *spi^{3}* or *aos$^{\Delta 7}$* mosaics appeared normal and exhibited two dorsal appendages (Table 2). Non-mosaic sibling controls produced virtually no intact eggs, confirming the penetrance of the *P[decDN]* collapsed egg phenotype (Table 2). Control females with the identical genotype, but in which mitotic recombination was not induced, produced no intact eggs, arguing that the presence of the mutant *rho*, *spi* or *aos* alleles did not alter the penetrance of the *P[decDN]* phenotype (see Table S1 in the supplementary material). Moreover, none of the collapsed eggs exhibited fused dorsal appendages (see Table S2 in the supplementary material), indicating that no patterning defects were overlooked owing to unanticipated problems with the *P[decDN]* marker. These data indicate that Spi-mediated autocrine amplification of Egfr signaling and Aos-mediated negative feedback are not required for eggshell patterning.

pnt is required for patterning of the dorsal follicular epithelium

We then took a candidate approach to identify additional genes involved in follicle cell patterning. We first looked at *pnt*, which encodes two Ets transcription factors, the expression of which is induced by Egfr activity in the ovary (Brunner et al., 1994; Gabay et al., 1996; Klambt, 1993; Morimoto et al., 1996; Rebay, 2002). Eggshells from *pnt* mutant epithelia exhibit a single dorsal eggshell appendage that is considerably wider than a wild-type appendage (Morimoto et al., 1996), but the requirement for *pnt* in the establishment of follicle cell fate had not been investigated.

Table 2. Frequency and appendage phenotype of intact eggs recovered from *P[decDN]* control and mosaic females

Genotype*	Total eggs	Intact eggs	Appendage phenotype % (*n*)				
			Wild-type	Partially fused	Completely fused	Further apart	None
TM3/P[decDN]118.3 FRT^{80B}	2166	0	n.a.	n.a.	n.a.	n.a.	n.a.
rho^{7M43} FRT^{80B}/P[decDN]118.3 FRT^{80B}	12,567	853	99.4 (848)	0.1 (1)	0 (0)	0 (0)	0.5 (4)
TM6B/P[decDN]118.3 FRT^{80B}	1674	0	n.a.	n.a.	n.a.	n.a.	n.a.
rho^{6} FRT^{80B}/P[decDN]118.3 FRT^{80B}	4351	31	96.8 (30)	0 (0)	0 (0)	0 (0)	3.2 (1)
CyO/P[decDN]006.1 FRT^{40A}	1912	0	n.a.	n.a.	n.a.	n.a.	n.a.
spi^{1} FRT^{40A}/P[decDN]006.1 FRT^{40A}	3224	58	100 (58)	0 (0)	0 (0)	0 (0)	0 (0)
CyO/P[decDN]006.1 FRT^{40A}	n.d.	0	n.a.	n.a.	n.a.	n.a.	n.a.
spi^{3} FRT^{40A}/P[decDN]006.1 FRT^{40A}	n.d.	91	100 (91)	0 (0)	0 (0)	0 (0)	0 (0)
TM3/P[decDN]172.1 FRT^{80B}	n.d.	2	100 (2)†	0 (0)	0 (0)	0 (0)	0 (0)
TM3/P[decDN]225.5 FRT^{80B}	4172	0	n.a.	n.a.	n.a.	n.a.	n.a.
aos$^{\Delta 7}$ FRT^{80B}/P[decDN]172.1 FRT^{80B}	n.d.	52	98.1 (51)‡	0 (0)	0 (0)	0 (0)	1.9 (1)
aos$^{\Delta 7}$ FRT^{80B}/P[decDN]225.5 FRT^{80B}	6192	46	97.8 (45)‡	0 (0)	0 (0)	0 (0)	2.2 (1)
TM3/FRT^{82B} P[decDN]2.129.3	1856	9§	100 (9)	0 (0)	0 (0)	0 (0)	0 (0)
FRT^{82B} pnt$^{\Delta 78}$/FRT^{82B} P[decDN]2.129.3	2152	37	27.0 (10)¶	10.8 (4)	62.2 (23)	0 (0)	0 (0)
TM3/FRT^{82B} P[decDN]140.1	n.d.	252§	100 (252)	0 (0)	0 (0)	0 (0)	0 (0)
TM3/FRT^{82B} P[decDN]140.4	n.d.	54§	100 (54)	0 (0)	0 (0)	0 (0)	0 (0)
FRT^{82B} pnt$^{\Delta 88}$/FRT^{82B} P[decDN]140.1	n.d.	402	7.7 (31)¶	6.7 (27)	83.1 (334)	0 (0)	2.5 (10)
FRT^{82B} pnt$^{\Delta 88}$/FRT^{82B} P[decDN]140.4	n.d.	175	21.7 (38)¶	19.4 (34)	54.9 (96)	0 (0)	4.0 (7)
TM6B/P[decDN]118.3 FRT^{80B}	5677	0	n.a.	n.a.	n.a.	n.a.	n.a.
TM6B/P[decDN]172.1 FRT^{80B}	n.d.	3§	100 (3)	0 (0)	0 (0)	0 (0)	0 (0)
TM6B/P[decDN]225.5 FRT^{80B}	n.d.	0	n.a.	n.a.	n.a.	n.a.	n.a.
mirr^{e48} FRT^{80B}/P[decDN]118.3 FRT^{80B}	5587	27**	18.5 (5)	0 (0)	0 (0)	0 (0)	63.0 (17)
mirr^{e48} FRT^{80B}/P[decDN]172.1 FRT^{80B}	n.d.	5	60.0 (3)¶	0 (0)	0 (0)	0 (0)	40.0 (2)
mirr^{e48} FRT^{80B}/P[decDN]225.5 FRT^{80B}	n.d.	7	0 (0)	0 (0)	0 (0)	0 (0)	100 (7)
TM6B/P[decDN]118.3 FRT^{80B}	7351	0	n.a.	n.a.	n.a.	n.a.	n.a.
sty$^{\Delta 5}$ FRT^{80B}/P[decDN]118.3 FRT^{80B}	n.d.	61	14.8 (9)††	0 (0)	0 (0)	85.2 (52)‡‡	0 (0)

*The beginning of each section lists the non-mosaic controls for *P[decDN]* penetrance, namely sibling females bearing a *P[decDN]* chromosome over a balancer chromosome.
†Appendages were wild-type in shape but appeared closer together.
‡Appendages were wild-type in shape but some appeared closer together, occasionally (10/51 and 1/45) the bases were touching.
§In this genetic background, the sibling controls displayed a background level of intact eggs, presumably owing to decreased penetrance of the *P[decDN]* effect. We therefore interpret these data in conjunction with the analysis of BR-C expression.
¶Given the complete penetrance of the effect of *pnt* or *mirr* follicle cell clones on BR-C expression, these wild-type eggs are likely to arise owing to incomplete penetrance of *P[decDN]* in this genetic background (see note above).
**Five eggs exhibited appendage phenotypes other than those listed in the column headings: three intact eggs had short thin appendages, one had three appendages, and one had one appendage shorter than the other.
††Appendages were wild-type distance apart, but some appeared mildly shorter in length or thicker in width.
‡‡In addition to the appendages being further apart than in wild type, most appeared mildly shorter in length or thicker in width, some had branched tips, and three eggs had a small pseudo-appendage at the base of one of their appendages.
n.a., not applicable. Eggshell phenotype is only scored for intact eggs.
n.d., not determined. The relevant information is the phenotype of the intact eggs, and so in some experiments the total number of eggs was not determined. However, for each genotype at least 2000 eggs in total were collected.

Intact eggshells produced by females mosaic for either *pnt$^{\Delta 78}$* or *pnt$^{\Delta 88}$* and bearing the *P[decDN]* marker exhibited a single thick appendage (Fig. 2B; Table 2). Unexpectedly, some intact eggs with a wild-type eggshell phenotype were also recovered. However, such eggs were also observed in the non-mosaic sibling controls (Table 2), suggesting that the penetrance of the *P[decDN]* collapsed egg phenotype was reduced in this genetic background and that these eggs were the products of non-mutant epithelia. Consistent with this interpretation, follicle cell fate defects associated with *pnt* mutant follicle cell clones are completely penetrant (see below). These data, together with previous observations (Morimoto et al., 1996), demonstrate that loss of *pnt* function in the follicular epithelium results in a loss of the appendage-free dorsal midline of the eggshell.

We then analyzed follicle cell fate directly and found that loss of *pnt* function from the dorsal midline region, which in the wild type lacks BR-C expression by stage 10B (Fig. 2C,C′), results in ectopic high-level BR-C expression indistinguishable from that observed within the appendage primordia (Fig. 2D-F″). This phenotype is completely penetrant (54/54 clones examined for *pnt$^{\Delta 88}$* and 30/30 clones for *pnt$^{\Delta 78}$*), and coincides precisely with the *pnt* clone borders (Fig. 2D″,E″,F″); even single-cell *pnt* mutant clones exhibited this effect on cell fate (Fig. 2F-F″). These data indicate that *pnt* function is required cell-autonomously to determine midline fate and that in the absence of *pnt*, the cells instead adopt an appendage-producing fate. Interestingly, the lack of BR-C expression in the operculum region is not affected by the loss of *pnt* (Fig. 2D-F″), indicating that this region is specified through a different mechanism than the dorsal midline, even though both exhibit identical BR-C levels.

In contrast to the dorsal midline, *pnt* mutant clones within the appendage primordia region had no effect on BR-C levels (Fig. 2D-F″). Interestingly, loss of *pnt* in follicle cells just posterior to the dorsal midline, which normally exhibit basal BR-C levels (Fig. 2C′), led to high BR-C levels, similar to those in the appendage primordia (Fig. 2E,E′). This effect was limited to the 2-3 rows of cells posterior to the normal primordia region, defining a domain within the follicular epithelium that is competent to adopt a primordium fate in the absence of *pnt*.

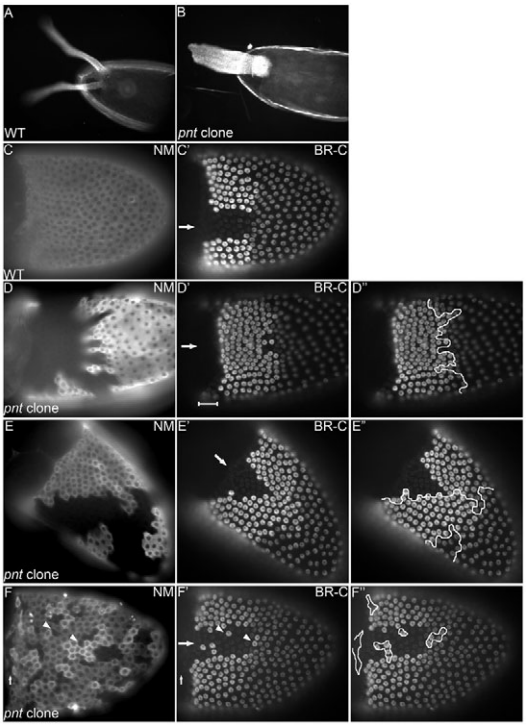

Fig. 2. Loss of *pnt* leads to cell-autonomous loss of dorsal midline follicle cell fate. *Drosophila* ovaries were stained for the NM clone marker (C-F) and for BR-C expression (C′-F′), and clone outlines were superimposed on the BR-C pattern (D″-F″). Arrows indicate the dorsal-most point of the egg chamber. (**A**) Eggshell from a complete wild-type follicle cell clone, marked by the absence of *P[decDN]*. (**B**) Eggshell from a complete *pnt* mutant follicle cell clone, marked by the absence of *P[decDN]*. (**C**,**C′**) Control stage 10B egg chamber from a *pnt* mosaic female, but lacking *pnt* mutant clones. (**D-D″**) Stage 11 egg chamber bearing a large *pnt* mutant clone involving most of the operculum/midline region and much of the appendage primordia. The operculum region (bar) is unaffected by the absence of *pnt*. (**E-E″**) Stage 10B egg chamber bearing a large *pnt* mutant clone involving a portion of one appendage primordium region, the dorsal midline region and some dorsal posterior cells. (**F-F″**) Stage 10B egg chamber bearing small *pnt* mutant clones. Small clones in the operculum region (small arrow) do not affect BR-C expression, whereas small clones in the midline (arrowheads) exhibit cell-autonomous ectopic high-level BR-C expression.

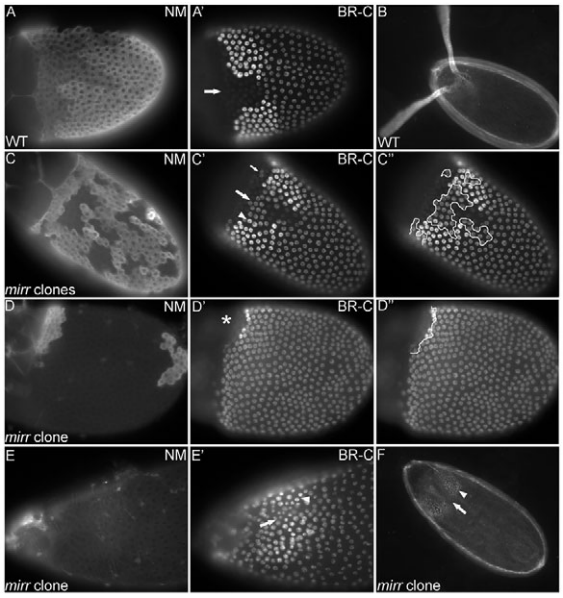

Fig. 3. Loss of *mirr* leads to a loss of all dorsal anterior follicle cell fates. *Drosophila* ovaries were stained for the NM clone marker (A,C,D,E) and for BR-C expression (A′,C′,D′,E′), and clone outlines were superimposed on the BR-C pattern (C″,D″). The dorsal midline is indicated (arrow). (**A**,**A′**) Stage 10B egg chamber from *mirr* mosaic females, but lacking dorsal *mirr* mutant clones. (**B**) Eggshell from a complete wild-type follicle cell clone, marked by the absence of *P[decDN]*. (**C-C″**) Stage 10B egg chamber with multiple small *mirr* mutant clones. Small arrow, clone in operculum region; arrowhead, occasional mutant cell in primordium region expressing high BR-C levels. (**D-D″**) Stage 10B egg chamber with large *mirr* mutant clones; the dorsal anterior is indicated (asterisk). (**E**,**E′**) Stage 13 egg chamber with large *mirr* mutant clone. The predicted position of the midline (arrow) and some nuclei with elevated BR-C levels (arrowhead) are indicated. (**F**) Eggshell from a complete *mirr* mutant follicle cell clone, marked by the absence of *P[decDN]*. Two domains of appendage-like imprints are visible (arrowhead) on either side of the dorsal-most region (arrow).

mirr is required for determination of midline- and appendage-producing fates

We next looked at the requirement for *mirr*, an Egfr target that encodes a homeodomain transcription factor expressed in dorsal anterior follicle cells during mid-oogenesis (Jordan et al., 2000; McNeill et al., 1997; Zhao et al., 2000). Loss of *mirr* has been associated with dorsal appendage defects, and ectopic *mirr* expression leads to ectopic high-level BR-C expression and ectopic appendage material (Atkey et al., 2006; Jordan et al., 2000; Zhao et al., 2000), but the changes in follicle cell patterning that lead to these defects have not been analyzed.

In contrast to the wild type (Fig. 3A,B), *mirr* mutant clones in the dorsal midline (Fig. 3C′, arrow) or operculum (Fig. 3C′, small arrow) regions failed to downregulate BR-C and instead exhibited a basal level of expression (Fig. 3C-D″). In the normal appendage primordia region, *mirr* mutant cells failed to upregulate BR-C, and thus also exhibited a basal level of BR-C expression, although the level was occasionally somewhat higher (Fig. 3C′, arrowhead). In all three regions, this effect was cell autonomous (Fig. 3C″,D″) (34/34). *mirr* mutant cells throughout the dorsal anterior region thus resemble ventral or posterior follicle cells that do not receive the Grk/Egfr signal, indicating that *mirr* is essential for determination of dorsal anterior fates. The fact that some cells in the primordia region can exhibit a mild elevation of BR-C expression, particularly in later stages (Fig. 3E,E′, arrowhead), suggests that this *mirr* allele is not a null, or that there is also a *mirr*-independent contribution to BR-C regulation in this region.

Consistent with this effect on follicle cell fate, the majority of intact eggshells produced by *mirr* mosaic females bearing the *P[decDN]* marker lacked dorsal appendages (Fig. 3F; Table 2). Intact eggs were recovered from these females at low frequency, likely reflecting the requirement for *mirr* in cyst encapsulation in early oogenesis, reducing the number of egg chambers with complete follicle cell clones that complete development (Jordan et al., 2000). Some eggs did exhibit appendages, possibly owing to decreased penetrance of the *P[decDN]* phenotype in this genetic background (see Discussion). Interestingly, eggs lacking appendages still retained a recognizable DV asymmetry in their shape (Fig. 3F, arrowhead), unlike the most severely affected eggs from *grk* mutant females (Schupbach, 1987), consistent with residual *mirr* activity or a possible *mirr*-independent contribution to follicle cell patterning (see above).

Because *mirr* and *pnt* have markedly different patterning phenotypes, it seems unlikely that they interact in a straightforward regulatory relationship. However, we found that expression of a *mirr* enhancer trap is decreased in *pnt* mutant follicle cells (see Fig. S1 in the supplementary material), suggesting that *mirr* is downstream of *pnt* and that *pnt* positively regulates *mirr* expression. Since *mirr* levels are highest at the dorsal midline in wild-type egg chambers (see Fig. S1 in the supplementary material) (Atkey et al., 2006), one interpretation is that *pnt* mutant cells at the dorsal midline fail to adopt a midline fate because they do not express sufficiently high levels of Mirr. In such a scenario, high Mirr levels would determine midline fate, whereas a broad range of lower *mirr* levels would determine appendage primordium fate. Mirr would thus play an important role as an effector of the Grk gradient.

sty is required for patterning of the dorsal follicular epithelium

The dynamic pattern of MAPK activation in the follicular epithelium during mid-oogenesis (Kagesawa et al., 2008; Nakamura and Matsuno, 2003; Peri et al., 1999; Wasserman and Freeman, 1998) is consistent with a decrease in Egfr activity at the dorsal midline during dorsal anterior patterning. We therefore looked at the requirement for *sty*, which is induced by Egfr activation and encodes an intracellular inhibitor of RTK signaling (Casci et al., 1999; Hacohen et al., 1998; Reich et al., 1999).

Follicular epithelia completely homozygous for the $sty^{\Delta 5}$ allele, or with large clones that included the entire dorsal anterior region, exhibited a pronounced increase in width along the DV axis of the dorsal midline domain (Fig. 4A-A″,C-C″, arrows) (9.6±0.3 cells versus 3.1±0.2 cells in non-mosaic egg chambers from the same females), as well as a reduction in the total number of cells per primordium (Fig. 4A-A″,C-C″) (28.2±1.6 cells versus 50.8±3.4 cells in controls). This lateral expansion of the dorsal midline domain can also be visualized by examining the apical distribution of the cell adhesion molecule Echinoid (Ed), which at these stages is cortically localized in all follicle cells except for those expressing high levels of BR-C (Fig. 4A″,C″, small arrows) (Laplante and Nilson, 2006).

These egg chambers also exhibited a reduction in the width along the DV axis of each appendage primordium (7.0±0.5 cells versus 8.8±0.3 cells in controls), suggesting that the cells within roughly the dorsal-most third of each presumptive primordium instead adopted a dorsal midline fate. Smaller *sty* mutant clones in this region also showed this phenotype (Fig. 4E-G″, arrowheads) and revealed that it is cell autonomous. Interestingly, when the border of such a clone fell within the dorsal region of the primordium, this cell fate change generated an ectopic midline region (Fig. 4E′,F′, arrowheads) flanked by two mini-primordia (Fig. 4E‴,F‴, arrows). Indeed, Ed staining revealed the apical constriction of these small, high-level BR-C-expressing domains, presumably as they prepared to produce appendages (Fig. 4F‴, arrows). Overall, the DV width of the dorsal domain (midline plus appendage primordia) was increased by about three cells in *sty* mutant epithelia, taking into account the increased width of the midline and the modest decrease in the width of the laterally shifted appendage primordia.

These *sty* mutant epithelia also exhibited changes in cell fate pattern along the AP axis. The AP length of the operculum domain of low BR-C expression (2.5±0.2 cells) was indistinguishable from that of non-mosaic controls (2.6±0.2 cells), but the posterior limit of the dorsal midline domain and appendage primordia was located more anteriorly (3.4±0.3 cells from the anterior, versus 5.9±0.2 cells in control egg chambers). This effect was seen most clearly in egg chambers in which roughly half of the dorsal anterior region was mutant, facilitating a direct comparison of wild-type and *sty* mutant regions within a single egg chamber (Fig. 4E-E″,G-G″, bars). This phenotype suggests that some cells in the posterior portion of the presumptive appendage primordia instead adopt a basal BR-C fate. Identical phenotypes were observed for the sty^{226} allele.

Consistent with this effect on follicle cell fate, intact eggshells produced by $sty^{\Delta 5}$ mosaic females bearing the *P[decDN]* marker exhibited an expanded dorsal midline region (Fig. 4B,D; Table 2) that was significantly wider than that of control eggs (57.3±2.3 μm versus 40.0±1.4 μm for intact eggs produced by wild-type mosaic females bearing the *P[decDN]* marker). Interestingly, the appendages of these eggshells did not appear dramatically reduced in size compared with the wild type, despite the reduced total

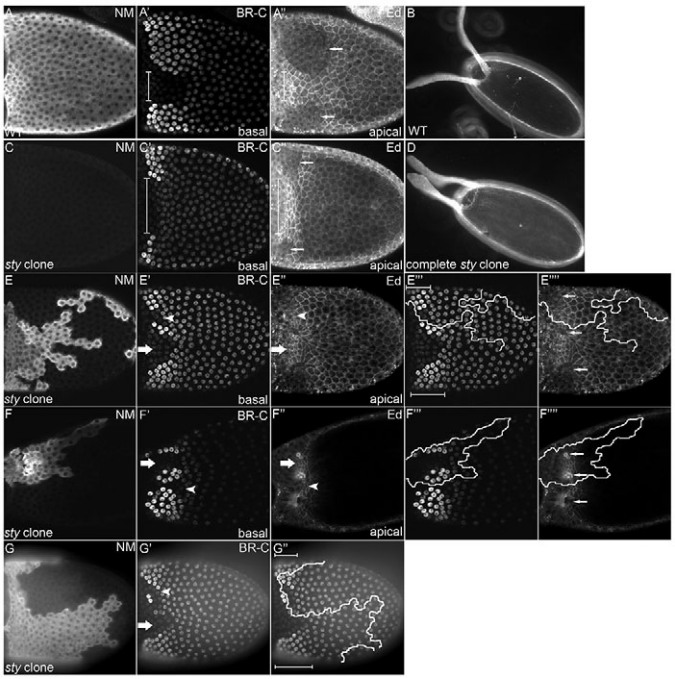

Fig. 4. Loss of *sty* leads to an altered pattern of dorsal anterior follicle cell fates. *Drosophila* ovaries were stained for the NM clone marker (A,C,E,F,G; basal sections), BR-C expression (A′,C′,E′,F′,G′; basal sections) and Ed expression (A″,C″, E″, F″; apical sections). Superimposed clone outlines are shown (E‴, E⁗, F‴, F⁗). Large arrows indicate the endogenous dorsal midline; arrowheads indicate ectopic midline fates; small arrows indicate appendage primordia. Bars indicate the AP extents of the endogenous and the DV extents of the ectopic primordia and midline regions. (**A-A″**) Stage 10B egg chamber from a *sty* mosaic female, but lacking *sty* mutant clones. (**B**) Eggshell from a complete wild-type follicle cell clone, marked by the absence of *P[decDN]*. (**C-C″**) Stage 10B egg chamber with a complete *sty* mutant clone. (**D**) Eggshell from a complete *sty* mutant follicle cell clone, marked by the absence of *P[decDN]*. (**E-E⁗**) Stage 10B egg chamber with a *sty* mutant clone involving part of one appendage primordium. The dorsal-most cells of the clone exhibit reduced BR-C expression (arrowhead). (**F-F⁗**) Stage 12 egg chamber with a *sty* mutant clone involving parts of both appendage primordia. (**G-G″**) Stage 10B egg chamber. Bars indicate the AP lengths of the wild-type (bottom) and mutant (top) primordia.

number of cells in the high-level BR-C-expressing domain, suggesting that morphogenesis might somehow compensate for the reduced number of cells.

DISCUSSION

Development of a dominant eggshell marker for follicle cell clones

As part of our analysis of patterning, we developed the *P[decDN]* marker, which allows the identification of laid eggs derived from egg chambers with homozygous mutant follicular epithelia. A recessive *dec-1* mutant allele was previously developed as an eggshell marker (Nilson and Schupbach, 1998) but is of limited utility for analysis of complete follicle cell clones because the mutant cells are marked by the production of defective eggshell. By contrast, in the *P[decDN]* system, the mutant cells are marked by the loss of *P[decDN]*, allowing us to recognize eggs that are the products of follicular epithelia that are largely or entirely mutant.

A potential complication of this system, not apparent in our initial tests (see Table 1), is the production of occasional intact eggshells by some negative control genotypes (see Table 2). Our current data suggest that certain *P[decDN]* transgenes exhibit a slightly decreased penetrance in certain genetic backgrounds. As discussed above, such low levels of background complicate, but do not prevent, the analysis of mutations associated with patterning defects, given that appropriate negative controls are included.

Rho, Spi and Aos are not required for patterning of the follicular epithelium

Our analysis of BR-C expression demonstrates that *rho*, *spi* and *aos* are not required for patterning of the dorsal anterior follicular epithelium, contrary to the current model of eggshell patterning (Wasserman and Freeman, 1998). Moreover, our analysis of mature eggshells using the *P[decDN]* eggshell marker revealed that loss of *rho*, *spi* or *aos* does not lead to eggshell patterning defects. Consistent with these data, eggs produced by *spi* mutant follicular epithelia bearing a recessive *dec-1* allele as an eggshell marker (Nilson and Schupbach, 1998) exhibit two normally positioned dorsal appendages (T. Schüpbach, personal communication). Collectively, these observations rule out a straightforward role for the Spi/Aos feedback loop in patterning of the dorsal anterior follicular epithelium.

Graded Egfr activity patterns the dorsal anterior follicular epithelium

In addition to our observations of *rho* and *spi* mutant clones, our data also argue more generally against the requirement for a diffusible factor that amplifies the Grk/Egfr signal. If Grk/Egfr signaling were to induce such a factor, then this induction would be predicted to increase in *sty* mutant clones, which presumably experience increased Egfr pathway activity. The increased production of the diffusible factor would be predicted to have non-autonomous effects on follicle cell fate, but *sty* clones have strictly cell-autonomous effects. Together, these data support a model in which spatial information is provided directly by the distribution of Grk, without induction of an intervening diffusible ligand. Consistent with this idea, recent analysis of internalization of Grk-Egfr complexes by the follicle cells, as well as quantitative modeling, indicate that the Grk signal extends at least to the lateral limits of the dorsal anterior domain (Chang et al., 2008; Goentoro et al., 2006).

According to such a model, midline fates are determined in cells that receive high levels of Grk/Egfr signaling, whereas appendage primordium fates are determined in cells that experience intermediate levels of signaling. This interpretation is supported by the distribution of Grk, which has a dorsal high point (Neuman-Silberberg and Schupbach, 1996), and the fact that a variety of manipulations that lead to increased Egfr activity, such as Grk overexpression or loss of negative regulators such as *sty*, *Cbl* or *kekkon-1*, lead to an expansion of dorsal midline fates (this study) (Ghiglione et al., 1999; Neuman-Silberberg and Schupbach, 1994; Pai et al., 2000; Zartman et al., 2009). Determination of distinct fates by distinct levels of Grk/Egfr signaling does not itself exclude a requirement for negative feedback in response to high-level Egfr signaling, but the observation that high levels of activated MAPK are restricted to the dorsal-most anterior follicle cells at the same time that BR-C is lost from the dorsal midline region (Kagesawa et al., 2008; Nakamura and Matsuno, 2003; Peri et al., 1999) suggests that feedback inhibition of Egfr activity is not required to specify dorsal midline fate.

Pnt is required cell-autonomously along the dorsal midline to repress appendage fate

A role for *pnt* in the specification of dorsal midline fate has been proposed previously (Morimoto et al., 1996; Yakoby et al., 2008b). Our clonal analysis demonstrates that *pnt* is required cell-autonomously in the dorsal midline domain to repress appendage primordium fate (Fig. 5A,C). Even single-cell *pnt* mutant clones exhibit ectopic, high BR-C levels, indicating that midline fate does not require *pnt*-mediated expression of a diffusible factor. Cells in the operculum region of the T-shaped operculum/midline domain are not affected by loss of *pnt* function, consistent with the presence of an operculum in the resulting eggshells. This differential effect of

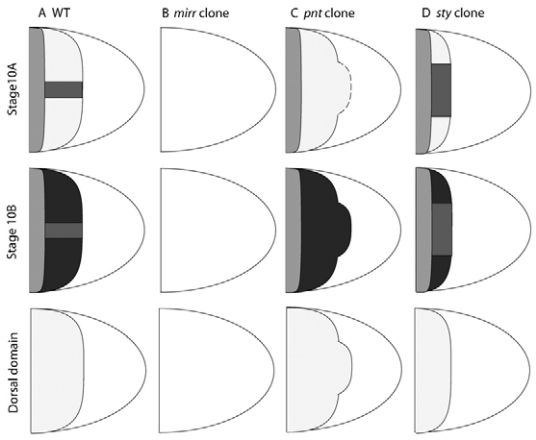

Fig. 5. Patterning of the dorsal anterior follicular epithelium downstream of Egfr. The operculum (light gray), midline (dark gray) and appendage primordium (black) fates are shown at stage 10A (top) and 10B (middle). The changes in the shape of the dorsal domain along the DV and AP axes are shown (bottom). (**A**) In the wild type (WT), the operculum and midline regions are detectable first, followed by the appendage primordium fate. (**B**) In the absence of *mirr*, the follicle cells do not acquire any of the dorsal fates. (**C**) In *pnt* clones, anterior-most follicle cells adopt operculum fates normally, but midline follicle cells fail to downregulate BR-C expression and instead adopt ectopic appendage fates. Dorsal follicle cells just posterior to the midline are also converted to appendage fates. (**D**) In *sty* mutant clones, the dorsolateral follicle cells closest to the midline adopt a midline fate, presumably owing to elevated Egfr signaling in the absence of *sty*. The AP length of the operculum domain is unaffected by the loss of *sty* but the AP length of the appendage primordia and midline domains is reduced.

loss of *pnt* function on the operculum and midline domains is consistent with the observation that Dpp signaling is required in the operculum region, but not in the midline, to downregulate BR-C (J.-F.B.L. and L.A.N., unpublished observations) (Yakoby et al., 2008b).

We also found that *pnt* is required to repress appendage primordium fate in the follicle cells just posterior to the dorsal midline domain, indicating that follicle cells posterior to the normal midline region are competent to adopt an appendage primordium fate (Fig. 5C). Loss of *pnt* thus converts two different domains to an appendage primordium fate, suggesting that Pnt interacts with different inputs and/or effectors in the normal dorsal midline region than in the cells just posterior to this region.

Mirr is required cell-autonomously for induction of all dorsal anterior fates

Our data demonstrate that *mirr* is required for determination of all dorsal anterior follicle cell fates (Fig. 5B). Loss of *grk* or *Egfr* function also leads to loss of these fates, and *mirr* is expressed in the dorsal anterior follicle cells in response to Grk/Egfr signaling (Jordan et al., 2000; Zhao et al., 2000). A straightforward interpretation of this phenotype is, therefore, that *mirr* is a critical target of Egfr signaling in dorsal anterior follicle cell fate determination, and that loss of *mirr* impairs the ability of the follicle cells to adopt the appropriate fate in response to the Grk/Egfr signal.

The *sty* mutant phenotype is consistent with increased Egfr signaling

sty mutant follicular epithelia exhibit an expanded dorsal midline region and a largely corresponding reduction in the DV width of the appendage primordia (Fig. 5D). Given the role of Sty as a negative regulator of RTK signaling, this shift in fates is consistent with a model in which high levels of Egfr signaling induce dorsal midline fate. However, the total extent of dorsal fates (midline plus primordia) along the DV axis exhibits a modest expansion at best, suggesting that patterning occurs within roughly the same domain along the DV axis, even though the distribution of cell fates within this region is markedly different. This observation might indicate that the slope of the Grk gradient is sharper near the lateral edges of this domain.

Unexpectedly, along the AP axis, loss of *sty* function leads to a reduction in the length of the primordia, suggesting that the profile of an AP determinant is affected, either directly or indirectly. The best candidate for such a determinant is Dpp, which influences follicle cell fate along the AP axis. Dpp is required to determine operculum fate (J.-F.B.L. and L.A.N., unpublished results) (Yakoby et al., 2008b), and Dpp overexpression, or removal of its negative regulator *brinker* (*brk*), causes an AP expansion of the operculum domain at the expense of appendage primordium fate (Chen and Schupbach, 2006; Deng and Bownes, 1997). The latter results seem to implicate Dpp in the repression of appendage fates, but some reports have concluded that appropriate levels of Dpp and Egfr activity cooperate to promote primordium fate (Peri and Roth, 2000; Shravage et al., 2007), whereas others have shown that loss of Dpp signaling does not affect this fate (J.-F.B.L. and L.A.N., unpublished results) (Yakoby et al., 2008b). Interestingly, more mild overexpression of Dpp seems to lead to a posterior shift of appendage primordium fates (Deng and Bownes, 1997; Dequier et al., 2001); whether these fates lie within the normal primordium region was not determined in these studies, but ectopic determination of primordium fate could suggest a role for Dpp beyond a repressive effect.

The AP defects in *sty* mutant clones cannot be explained by a simple model in which high levels of Egfr signaling cooperate with Dpp to induce dorsal anterior fates. Given the apparent DV expansion of the domain of high-level Egfr signaling, one would predict an expansion or no effect. Instead, the AP length of primordia is decreased, whereas the length of the operculum domain along the AP axis is unaffected. Another possible explanation is that the loss of *sty* function leads to decreased Dpp signaling. For example, Egfr activation induces the expression of *brk* (Campbell and Tomlinson, 1999; Chen and Schupbach, 2006; Minami et al., 1999; Shravage et al., 2007), suggesting that increased Egfr signaling in *sty* mutant epithelia might lead to ectopic *brk* expression, which in turn would modify the profile of the Dpp gradient and alter patterning along the AP axis. Alternatively, increased Egfr activity could impact Dpp signaling at another level of the pathway, or loss of *sty* could influence an as yet unrecognized determinant of appendage primordium fate.

Together, our data support a model in which graded Grk/Egfr signaling determines distinct dorsal anterior cell fates without a requirement for intervening autocrine feedback. Moreover, the changes in cell fate we observe in various mutant conditions reveal the ways in which the pattern can be altered, which is itself informative. The identification and characterization of such shifts in cell fate pattern, using BR-C and other markers, will contribute to the dissection of the spatial and temporal components that pattern this tissue during this developmental period.

Acknowledgements

We thank Gail Waring for providing *P[decDN]* reagents prior to publication; Nam Sung Moon, Siegfried Roth, Hannele Ruohola-Baker, Trudi Schüpbach and the Developmental Studies Hybridoma Bank for reagents; Wei-Ju Chen, Hana Dembe, Samantha Man, Alysha Manji, Kari McKinley and Fazmina Zamzameer for help with experiments; Trudi Schüpbach and Stas Shvartsman for sharing unpublished data; and Trudi Schüpbach, Frieder Schöck and Chiara Gamberi for helpful comments on the manuscript. This research was funded by the Canadian Cancer Society, the Natural Sciences and Engineering Research Council of Canada, and the Canadian Institutes of Health Research. L.A.N. was supported by the Canada Research Chairs Program.

Supplementary material

Supplementary material for this article is available at
http://dev.biologists.org/cgi/content/full/136/17/2893/DC1

References

Atkey, M. R., Lachance, J. F., Walczak, M., Rebello, T. and Nilson, L. A. (2006). Capicua regulates follicle cell fate in the Drosophila ovary through repression of mirror. *Development* **133**, 2115-2123.

Bauer, B. J. and Waring, G. L. (1987). 7C female sterile mutants fail to accumulate early eggshell proteins necessary for later chorion morphogenesis in Drosophila. *Dev. Biol.* **121**, 349-358.

Berg, C. A. (2005). The Drosophila shell game: patterning genes and morphological change. *Trends Genet.* **21**, 346-355.

Brunner, D., Ducker, K., Oellers, N., Hafen, E., Scholz, H. and Klambt, C. (1994). The ETS domain protein pointed-P2 is a target of MAP kinase in the sevenless signal transduction pathway. *Nature* **370**, 386-389.

Campbell, G. and Tomlinson, A. (1999). Transducing the Dpp morphogen gradient in the wing of Drosophila: regulation of Dpp targets by brinker. *Cell* **96**, 553-562.

Casci, T., Vinos, J. and Freeman, M. (1999). Sprouty, an intracellular inhibitor of Ras signaling. *Cell* **96**, 655-665.

Chang, W. L., Liou, W., Pen, H. C., Chou, H. Y., Chang, Y. W., Li, W. H., Chiang, W. and Pai, L. M. (2008). The gradient of Gurken, a long-range morphogen, is directly regulated by Cbl-mediated endocytosis. *Development* **135**, 1923-1933.

Chen, Y. and Schupbach, T. (2006). The role of brinker in eggshell patterning. *Mech. Dev.* **123**, 395-406.

Chou, T. B. and Perrimon, N. (1992). Use of a yeast site-specific recombinase to produce female germline chimeras in Drosophila. *Genetics* **131**, 643-653.
Chou, T. B. and Perrimon, N. (1996). The autosomal FLP-DFS technique for generating germline mosaics in Drosophila melanogaster. *Genetics* **144**, 1673-1679.
Deng, W. M. and Bownes, M. (1997). Two signalling pathways specify localised expression of the Broad-Complex in Drosophila eggshell patterning and morphogenesis. *Development* **124**, 4639-4647.
Dequier, E., Souid, S., Pal, M., Maroy, P., Lepesant, J. A. and Yanicostas, C. (2001). Top-DER- and Dpp-dependent requirements for the Drosophila fos/kayak gene in follicular epithelium morphogenesis. *Mech. Dev.* **106**, 47-60.
DiBello, P. R., Withers, D. A., Bayer, C. A., Fristrom, J. W. and Guild, G. M. (1991). The Drosophila Broad-Complex encodes a family of related proteins containing zinc fingers. *Genetics* **129**, 385-397.
Dorman, J. B., James, K. E., Fraser, S. E., Kiehart, D. P. and Berg, C. A. (2004). bullwinkle is required for epithelial morphogenesis during Drosophila oogenesis. *Dev. Biol.* **267**, 320-341.
Gabay, L., Scholz, H., Golembo, M., Klaes, A., Shilo, B. Z. and Klambt, C. (1996). EGF receptor signaling induces pointed P1 transcription and inactivates Yan protein in the Drosophila embryonic ventral ectoderm. *Development* **122**, 3355-3362.
Ghiglione, C., Carraway, K. L., 3rd, Amundadottir, L. T., Boswell, R. E., Perrimon, N. and Duffy, J. B. (1999). The transmembrane molecule kekkon 1 acts in a feedback loop to negatively regulate the activity of the Drosophila EGF receptor during oogenesis. *Cell* **96**, 847-856.
Goentoro, L. A., Reeves, G. T., Kowal, C. P., Martinelli, L., Schupbach, T. and Shvartsman, S. Y. (2006). Quantifying the Gurken morphogen gradient in Drosophila oogenesis. *Dev. Cell* **11**, 263-272.
Goff, D. J., Nilson, L. A. and Morisato, D. (2001). Establishment of dorsal-ventral polarity of the Drosophila egg requires capicua action in ovarian follicle cells. *Development* **128**, 4553-4562.
Hacohen, N., Kramer, S., Sutherland, D., Hiromi, Y. and Krasnow, M. A. (1998). sprouty encodes a novel antagonist of FGF signaling that patterns apical branching of the Drosophila airways. *Cell* **92**, 253-263.
Hawley, R. J. and Waring, G. L. (1988). Cloning and analysis of the dec-1 female-sterile locus, a gene required for proper assembly of the Drosophila eggshell. *Genes Dev.* **2**, 341-349.
Horne-Badovinac, S. and Bilder, D. (2005). Mass transit: epithelial morphogenesis in the Drosophila egg chamber. *Dev. Dyn.* **232**, 559-574.
Jordan, K. C., Clegg, N. J., Blasi, J. A., Morimoto, A. M., Sen, J., Stein, D., McNeill, H., Deng, W. M., Tworoger, M. and Ruohola-Baker, H. (2000). The homeobox gene mirror links EGF signalling to embryonic dorso-ventral axis formation through notch activation. *Nat. Genet.* **24**, 429-433.
Kagesawa, T., Nakamura, Y., Nishikawa, M., Akiyama, Y., Kajiwara, M. and Matsuno, K. (2008). Distinct activation patterns of EGF receptor signaling in the homoplastic evolution of eggshell morphology in genus Drosophila. *Mech. Dev.* **125**, 1020-1032.
Klambt, C. (1993). The Drosophila gene pointed encodes two ETS-like proteins which are involved in the development of the midline glial cells. *Development* **117**, 163-176.
Klein, D. E., Nappi, V. M., Reeves, G. T., Shvartsman, S. Y. and Lemmon, M. A. (2004). Argos inhibits epidermal growth factor receptor signalling by ligand sequestration. *Nature* **430**, 1040-1044.
Laplante, C. and Nilson, L. A. (2006). Differential expression of the adhesion molecule Echinoid drives epithelial morphogenesis in Drosophila. *Development* **133**, 3255-3264.
McNeill, H., Yang, C. H., Brodsky, M., Ungos, J. and Simon, M. A. (1997). mirror encodes a novel PBX-class homeoprotein that functions in the definition of the dorsal-ventral border in the Drosophila eye. *Genes Dev.* **11**, 1073-1082.
Minami, M., Kinoshita, N., Kamoshida, Y., Tanimoto, H. and Tabata, T. (1999). brinker is a target of Dpp in Drosophila that negatively regulates Dpp-dependent genes. *Nature* **398**, 242-246.
Morimoto, A. M., Jordan, K. C., Tietze, K., Britton, J. S., O'Neill, E. M. and Ruohola-Baker, H. (1996). Pointed, an ETS domain transcription factor, negatively regulates the EGF receptor pathway in Drosophila oogenesis. *Development* **122**, 3745-3754.
Nakamura, Y. and Matsuno, K. (2003). Species-specific activation of EGF receptor signaling underlies evolutionary diversity in the dorsal appendage number of the genus Drosophila eggshells. *Mech. Dev.* **120**, 897-907.
Neuman-Silberberg, F. S. and Schupbach, T. (1993). The Drosophila dorsoventral patterning gene gurken produces a dorsally localized RNA and encodes a TGF alpha-like protein. *Cell* **75**, 165-174.
Neuman-Silberberg, F. S. and Schupbach, T. (1994). Dorsoventral axis formation in Drosophila depends on the correct dosage of the gene gurken. *Development* **120**, 2457-2463.
Neuman-Silberberg, F. S. and Schupbach, T. (1996). The Drosophila TGF-alpha-like protein Gurken: expression and cellular localization during Drosophila oogenesis. *Mech. Dev.* **59**, 105-113.
Nilson, L. A. and Schupbach, T. (1998). Localized requirements for windbeutel and pipe reveal a dorsoventral prepattern within the follicular epithelium of the Drosophila ovary. *Cell* **93**, 253-262.
Nilson, L. A. and Schupbach, T. (1999). EGF receptor signaling in Drosophila oogenesis. *Curr. Top. Dev. Biol.* **44**, 203-243.
O'Neill, E. M., Rebay, I., Tjian, R. and Rubin, G. M. (1994). The activities of two Ets-related transcription factors required for Drosophila eye development are modulated by the Ras/MAPK pathway. *Cell* **78**, 137-147.
Pai, L. M., Barcelo, G. and Schupbach, T. (2000). D-cbl, a negative regulator of the Egfr pathway, is required for dorsoventral patterning in Drosophila oogenesis. *Cell* **103**, 51-61.
Peri, F. and Roth, S. (2000). Combined activities of Gurken and decapentaplegic specify dorsal chorion structures of the Drosophila egg. *Development* **127**, 841-850.
Peri, F., Bokel, C. and Roth, S. (1999). Local Gurken signaling and dynamic MAPK activation during Drosophila oogenesis. *Mech. Dev.* **81**, 75-88.
Preston, C. R. and Engels, W. R. (1996). P-element-induced male recombination and gene conversion in Drosophila. *Genetics* **144**, 1611-1622.
Rebay, I. (2002). Keeping the receptor tyrosine kinase signaling pathway in check: lessons from Drosophila. *Dev. Biol.* **251**, 1-17.
Reich, A., Sapir, A. and Shilo, B. (1999). Sprouty is a general inhibitor of receptor tyrosine kinase signaling. *Development* **126**, 4139-4147.
Scholz, H., Deatrick, J., Klaes, A. and Klambt, C. (1993). Genetic dissection of pointed, a Drosophila gene encoding two ETS-related proteins. *Genetics* **135**, 455-468.
Schupbach, T. (1987). Germ line and soma cooperate during oogenesis to establish the dorsoventral pattern of egg shell and embryo in Drosophila melanogaster. *Cell* **49**, 699-707.
Schupbach, T., Clifford, R. J., Manseau, L. and Price, J. V. (1991). Dorsoventral signaling processes in Drosophila oogenesis. In *Cell-Cell Interactions in Early Development* (ed. J. Gerhart), pp. 163-174. New York: Wiley-Liss.
Shravage, B. V., Altmann, G., Technau, M. and Roth, S. (2007). The role of Dpp and its inhibitors during eggshell patterning in Drosophila. *Development* **134**, 2261-2271.
Spangenberg, D. K. and Waring, G. L. (2007). A mutant dec-1 transgene induces dominant female sterility in Drosophila melanogaster. *Genetics* **177**, 1595-1608.
Spradling, A. C. (1993). Developmental Genetics of Oogenesis. In *The Development of Drosophila melanogaster*, vol. 1 (ed. M. Bate and A. Martinez Arias), pp. 1-70. Cold Spring Harbor, NY: Cold Spring Harbor Laboratory Press.
Stein, D., Roth, S., Vogelsang, E. and Nusslein-Volhard, C. (1991). The polarity of the dorsoventral axis in the Drosophila embryo is defined by an extracellular signal. *Cell* **65**, 725-735.
Sturtevant, M. A., Roark, M. and Bier, E. (1993). The Drosophila rhomboid gene mediates the localized formation of wing veins and interacts genetically with components of the EGF-R signaling pathway. *Genes Dev.* **7**, 961-973.
Twombly, V., Blackman, R. K., Jin, H., Graff, J. M., Padgett, R. W. and Gelbart, W. M. (1996). The TGF-beta signaling pathway is essential for Drosophila oogenesis. *Development* **122**, 1555-1565.
Tzolovsky, G., Deng, W. M., Schlitt, T. and Bownes, M. (1999). The function of the broad-complex during Drosophila melanogaster oogenesis. *Genetics* **153**, 1371-1383.
Voas, M. G. and Rebay, I. (2003). The novel plant homeodomain protein rhinoceros antagonizes Ras signaling in the *Drosophila* eye. *Genetics* **165**, 1993-2006.
Wasserman, J. D. and Freeman, M. (1998). An autoregulatory cascade of EGF receptor signaling patterns the Drosophila egg. *Cell* **95**, 355-364.
Xu, T. and Rubin, G. M. (1993). Analysis of genetic mosaics in developing and adult Drosophila tissues. *Development* **117**, 1223-1237.
Yakoby, N., Bristow, C. A., Gong, D., Schafer, X., Lembong, J., Zartman, J. J., Halfon, M. S., Schupbach, T. and Shvartsman, S. Y. (2008a). A combinatorial code for pattern formation in Drosophila oogenesis. *Dev. Cell* **15**, 725-737.
Yakoby, N., Lembong, J., Schupbach, T. and Shvartsman, S. Y. (2008b). Drosophila eggshell is patterned by sequential action of feedforward and feedback loops. *Development* **135**, 343-351.
Zartman, J. J., Kanodia, J. S., Cheung, L. S. and Shvartsman, S. Y. (2009). Feedback control of the EGFR signaling gradient: superposition of domain-splitting events in *Drosophila* oogenesis. *Development* **136**, 2903-2911.
Zhao, D., Woolner, S. and Bownes, M. (2000). The Mirror transcription factor links signalling pathways in Drosophila oogenesis. *Dev. Genes Evol.* **210**, 449-457.

Table S1. Frequency and appendage phenotype of intact eggs recovered from *P[decDN]* females in the absence of heat-shock-induced mitotic recombination

Genotype	Total eggs	Intact % (*n*)	Appendage phenotype			
			Wild type	Bases touching	Partially fused	Completely fused
rho^{7M43} *FRT*^{80B}/ *P[decDN]118.3 FRT*^{80B}	1223	0 (0)	n.a.	n.a.	n.a.	n.a.
aos$^{\Delta 7}$ *FRT*^{80B}/ *P[decDN]172.1 FRT*^{80B}	1565	0.2 (3)	1	1	1	0
aos$^{\Delta 7}$ *FRT*^{80B}/ *P[decDN]225.5 FRT*^{80B}	3525	0.06 (2)	2	0	0	0

n.a., not applicable. Eggshell phenotype is only scored for intact eggs.

Table S2. Appendage phenotype of *P[decDN]* collapsed eggs recovered from mosaic females

Genotype	Collapsed eggs*	Appendage phenotype % (*n*)				
		Separate bases	Bases touching	Partially fused	Completely fused	None or reduced
FRT^{80B}/ P[decDN]118.3 FRT^{80B}	318	98.8 (314)	0.6 (2)	0 (0)	0 (0)	0.6 (2)
FRT^{82B} pnt$^{\Delta 78}$/ FRT^{82B} P[decDN]2.129.3	254	81.5 (207)	0 (0)	7.5 (19)	10.2 (26)	0.8 (2)
mirr^{e48} FRT^{80B}/ P[decDN]225.5 FRT^{80B}	255	92.9 (237)	0 (0)	0 (0)	0(0)	7.1 (18)
rho^{7M43} FRT^{80B}/ P[decDN]118.3 FRT^{80B}	244	94.7 (231)	0.4 (1)	0 (0)	0 (0)	4.9 (12)
spi^{1} FRT^{40A}/ P[decDN]006.1 FRT^{40A}	238	100 (238)	0 (0)	0 (0)	0 (0)	0 (0)
aos$^{\Delta 7}$ FRT^{80B}/ P[decDN]172.1 FRT^{80B}	332	92.8 (308)	3.3 (11)	0 (0)	0 (0)	3.9 (13)
aos$^{\Delta 7}$ FRT^{80B}/ P[decDN]225.5 FRT^{80B}	240	98.8 (237)	0.8 (2)	0 (0)	0 (0)	0.4 (1)

*A random sample of collapsed eggs was analyzed for each genotype.